Title
Timemresolved fluorescence of S-100a protein: effect of Ca+, Mg2+ and unilamellar vesicles of egg phosphatidylcholine

Journal
Cell Calcium, 20(6)

ISSN
0143-4160

Authors
Zolese, Giovanna
Giambanco, Ileana
Curatola, Giovanna
et al.

Publication Date
1996-12-01

DOI
10.1016/s0143-4160(96)90088-3

Cell Calcium (1996) 20(6), 465–474

Time-resolved fluorescence of S-100a protein: effect of Ca^{2+}, Mg^{2+} and unilamellar vesicles of egg phosphatidylcholine

Giovanna Zolese[1], Ileana Giambanco[2], Giovanna Curatola[1], Roberto Staffolani[1], Enrico Gratton[3], Rosario Donato[2]

[1]Istituto di Biochimica, Facoltà di Medicina, Università di Ancona, Ancona, Italy
[2]Department of Experimental Medicine and Biochemical Sciences, Section of Anatomy, University of Perugia, Perugia, Italy
[3]Laboratory for Fluorescence Dynamics, University of Illinois, Urbana, Illinois, USA

Summary Phase-modulation fluorescence lifetime measurements were used to study the single Trp residue of the Ca^{2+}-binding protein S-100a both in the absence and in the presence of Ca^{2+} and/or Mg^{2+}. Trp fluorescence decay for the protein was satisfactorily described by Lorentzian lifetime distributions centered around two components (approximately 4 ns and 0.5 ns). Lifetime values were unchanged by 2 mM Ca^{2+}, but the fractional intensity associated with longer lifetime increased up to 75%. In the presence of Mg^{2+}, the Ca^{2+} induced increase of the fractional intensity associated with longer lifetime was only 57%. For the protein in buffer, about the 85% of the recovered anisotropy was associated to a rotational correlation time of 6.7 ns. After the addition of Ca^{2+}, this value was increased to 16.08 ns. In the presence of Mg^{2+}, Ca^{+2} increased the rotational correlation time to 33.75 ns. Similar studies were performed with S-100a interacting with egg phosphatidylcholine vesicles (SUV). Our data suggest that the conformation of the protein may be influenced by structural features of the lipidic membrane. Moreover, data obtained in the presence of Mg^{2+} indicate some interaction between lipids and S-100, likely mediated by this ion.

INTRODUCTION

S-100a is the αβ isoform of S-100 protein, a group of closely related, 21 kDa, acidic Ca^{2+}-binding proteins (S-100ao, S-100a and S-100b) [1] belonging to the superfamily of Ca^{2+}-binding proteins of EF-hand type. Calmodulin, troponin C and parvalbumin belong to the same family and exhibit a common structural motif, the EF-hand which binds Ca^{2+} with high affinity [2,3]. In S-100, the 30 residue putative 'EF-hand' Ca^{2+}-binding domain (site I), is located in the C-terminal part of both α and β subunits. A non-conventional Ca^{2+}-binding site (28 residues) (site II) is localized in the N-terminus of individual chains. The α subunit of S100 is characterized by a single Trp residue (Trp 90) located in the C-terminus of the polypeptide [4]. This Trp residue belongs to an hydrophobic sequence, containing Trp-90, Phe-88, Phe-89, Cys-84 and Tyr-73 [5]. This sequence might constitute the α helix (helix D) essential for the Ca^{2+}-binding domain of the site II [5]. Many spectral studies have shown Ca^{2+}-binding induced conformational changes in these proteins, such as a decrease in α helical content [6]. Moreover, for S-100a, it has been shown that Trp moves to a more polar environment in the presence of saturating amounts of Ca^{2+} [6–8]. S-100 proteins are found in a soluble and a membrane-bound form and have the ability to interact with artificial and natural membranes [1,9–11]. Modulatory effects of S-100

Received 27 March 1996
Revised 9 August 1996
Accepted 23 August 1996

Correspondence to: Dr Giovanna Zolese, Istituto di Biochimica, Facoltà di Medicina e Chirurgia, Università degli Studi di Ancona, Via Ranieri, 60131 Ancona, Italy
Tel. +39 71 220 4673: Fax. +39 71 220 4398

proteins on some membrane protein activities have been demonstrated [1], although direct interactions with proteins or with their microenvironment remain to be elucidated. In the present work, the intrinsic fluorescence of S-100a was studied by time-resolved techniques. The Trp fluorescence decay data were acquired by a frequency domain fluorometer and were analyzed either in terms of exponential decay or as continuous distributions of lifetime values [12]. According to the approach proposed by Alcala et al. [12], it is assumed that the proteins can exhibit a large number of conformations and that the rate of interconversion between them can be of the same order of magnitude as that of the excited-state decay rate. In the distributional model, this could result in a large distribution of Trp lifetimes, due to the different microenvironments sampled during the excited state. The aim of the present work is to establish how the interaction of S-100a with Ca^{+2}, Mg^{2+} or phospholipids affects the decay pattern of the Trp emission, in order to understand some molecular details concerning the S-100a-membrane interactions. Fluorescence anisotropy measurements provide additional information about the rotational mobility of the residues in the absence or in the presence of ions and/or lipid vesicles.

MATERIALS AND METHODS

Protein purification

S-100a was purified by bovine brain as previously described [13].

Sample preparation

Egg phosphatidylcholine (EPC: Avanti Polar, Birmingham, AL, USA), suspended in chloroform, was dried under nitrogen flux in a round bottom flask. Small unilamellar vesicles (SUV) were formed by resuspending lipids, at 35°C, in 25 mM Tris/HCl, 0.1 mM EDTA, pH 7.4 (when necessary 5 mM Mg^{2+} was included in the buffer), at a concentration of 1 mg/ml and sonicating to clarification in a bath-type sonicator. Before each measurement, the lipid was incubated at 20°C for 1 h with the protein. The final concentrations of the lipid and S-100a in the sample were 0.2 mM and 14 μM, respectively. When present, Ca^{2+} and Mg^{2+} were 2 mM and 5 mM, respectively.

Time-resolved fluorescence measurements

The decay of S100a protein was studied by a multifrequency phase fluorometer, at the Laboratory for Fluorescence Dynamics (LFD), University of Illinois at Urbana-Champaign (IL, USA), using the harmonic content of a Coherent Antares Model mode-locked, synchronously pumped, cavity-dumped, and externally frequency-doubled dye laser. Excitation was at 295 nm using magic angle configuration, and the emission was observed through an optical filter combination of UV34 and U340 (from Oriel Corp.) chosen to select a band centered at 355 nm, in the range 320–380 nm. A solution of *p*-terphenyl in cyclohexane (lifetime 1.05 ns) was used as reference. The modulation frequency was varied from 2–350 MHz. Data were acquired at 14 different frequencies with the uncertainties of 0.2° and 0.004 for phase angles and modulation ratios, respectively. Anisotropy decay data were acquired with the same set of frequencies, using an excitation wavelength of 295 nm. Fluorescence decay data were fitted to a sum of exponential decay components using a non-linear least square analysis or as continuous distributions of lifetime values. The analysis software for lifetime and anisotropy determinations was provided by ISS Inc. according to models and equations described by Alcala et al. [11]. The reduced X^2 value was used to judge the goodness of fit [11]. All measurements were performed at 18°C.

RESULTS

Fluorescence decay measurement

The fluorescence decay of S-100a was measured at 18°C both in the presence and in the absence of 2 mM Ca^{2+}. Tables 1 and 2 report tryptophanyl emission decay of S-100a analyzed as a sum of a discrete number of exponential components (Table 1) or in terms of continuous Lorentzian lifetime distributions (Table 2). The biexponential analysis results (Table 1) are in agreement with our previous data [13]. However, data obtained are better described as a sum of three exponentials and the contribution of the fraction of shorter lifetimes is noticeable. Differences between the present measurements and our previous data [13] are likely to be ascribed to better resolution due to the different number and set of frequencies used [11]. Table 1 reports the effects of divalent cations (Ca^{2+} and/or Mg^{2+}) on fluorescence decay of S-100a in buffer. When present, Ca^{2+} and Mg^{2+} were 2 mM and 5 mM, respectively. Using the exponential analysis, the best results were obtained by a three exponential fit, showing that the cations induce modifications on the lifetime values and on the fractional intensity linked to τ_1 (f_1) and to the shorter lifetime value (f_3). Also, double exponential analysis shows a Ca^{2+} induced increase of the fractional intensity at the longer lifetime. These results are in agreement with data of Baudier et al. [14], Wang et al. [16] and with our previous work [13]. The three exponentials fit shows a Ca^{2+} induced increase of f_1 (from 0.3 to 0.55, +83%). The f_3 behaves almost in a complementary manner (from 0.35 to 0.09, −74%).

Table 1 Fluorescence decay fitting parameters for S-100a in buffer. Fluorescence decay was measured at 18°C, with an excitation wavelength of 295 nm. When present, Ca^{2+} and Mg^{2+} were 2 mM and 5 mM, respectively. Data were fitted to a sum of exponential decay components

	τ_1	f_1	τ_2	f_2	τ_3	f_3	X^2
S100a	0.98	1					1395
	3.51	0.49	0.47	0.51			16
	5.09	0.30	1.40	0.35	0.35	0.35	0.43
+Ca^{2+}	2.56	1					1288
	4.09	0.82	0.54	0.18			25
	5.43	0.55	2.01	0.36	0.31	0.09	0.92
+Mg^{2+}	1.08	1					1510
	3.83	0.50	0.50	0.50			18
	5.55	0.31	1.51	0.34	0.38	0.35	0.98
+Mg^{2+} + Ca^{2+}	2.23	1					1550
	4.14	0.76	0.57	0.24			25.5
	5.61	0.50	1.92	0.37	0.35	0.13	0.39

τ_1, τ_2, τ_3 lifetime values (ns); f_1, f_2, f_3 fluorescence fractions; X^2, reduced chi-square. For other experimental details, *see* Materials and Methods.

Moreover changes in τ_i, more evident for τ_2 (from 1.40 ns to 2.01 ns, +44%), are measured. The presence of 5 mM Mg^{2+} induces only slight modifications on the three exponentials fit of data, in line with previous results [15]. The addition of Ca^{2+} in the sample containing Mg^{2+} induces significant changes in the decay parameters, but less evident than those obtained in the absence of this cation (f_1 shows a 67% increase and f_3 a 63% decrease). Similar results were obtained using a Lorentzian distributional analysis (Table 2). Gaussian and Uniform distribution analysis did not yet good fits for the same data, in agreement with a previous work [13]. Figures 1 and 2 show representative multifrequency phase and modulation data for S-100a in the presence of 2 mM Ca^{2+} (Fig. 1) and of 2 mM Ca^{2+} and 5 mM Mg^{2+} (Fig. 2). The data were well fitted either with a three exponential function (Fig. 1B and Fig. 2B) or with a two continuous Lorentzian distribution of lifetimes (Fig. 1D and Fig. 2D), showing almost similar randomly distributed deviations between measured and calculated values (Fig. 1A,C and Fig. 2A,C). Since it is difficult to compare the fitted τ_i and f_i, we fitted the data to a two components continuous (Lorentzian) distribution of lifetimes, in order to compare these results with previous data [13]. Such distribution fits yield X^2 values comparable to those obtained by the three exponentials fit, and were here used as an alternative fitting procedure. At 18°C, the fluorescence decay of S-100a in the absence of Ca^{2+} was characterized by broad distributions of lifetimes (w), centered at 3.90 ns and 0.55 ns, and associated with fractional intensities of 35% and 65%, respectively. The presence of Ca^{2+} did not significantly change the lifetime values (4.03 ns and 0.52 ns, respectively), but increased the fractional intensity associated with longer lifetime up to 75%. Moreover, at the temperature used for the

Table 2 Fluorescence decay fitting parameters for S-100a in buffer. Fluorescence decay was measured at 18°C, with an excitation wavelength of 295 nm. When present, Ca^{2+} and Mg^{2+} were 2 mM and 5 mM, respectively. Data were fitted as Lorentzian continuous distributions of lifetime values

	c_1	w_1	f_1	c_2	w_2	f_2	X^2
S100a	0.44	2.38	1				18
	3.90	0.83	0.35	0.55	0.65	0.65	0.92
+Ca^{2+}	2.54	4.12	1				66
	4.03	1.08	0.75	0.52	1.87	0.25	2.5
+Mg^{2+}	0.49	2.67	1				19
	4.10	1.26	0.40	0.59	0.61	0.60	1.0
+Mg^{2+} + Ca^{2+}	2.00	4.32	1				53
	4.41	0.57	0.57	0.80	2.05	0.43	1.56

f_1, f_2, f_3 fluorescence fractions; c_1, c_2, w_1, w_2, centers and widths of Lorentzian distributions, respectively; X^2, reduced chi-square.For other experimental details, *see* Materials and methods.

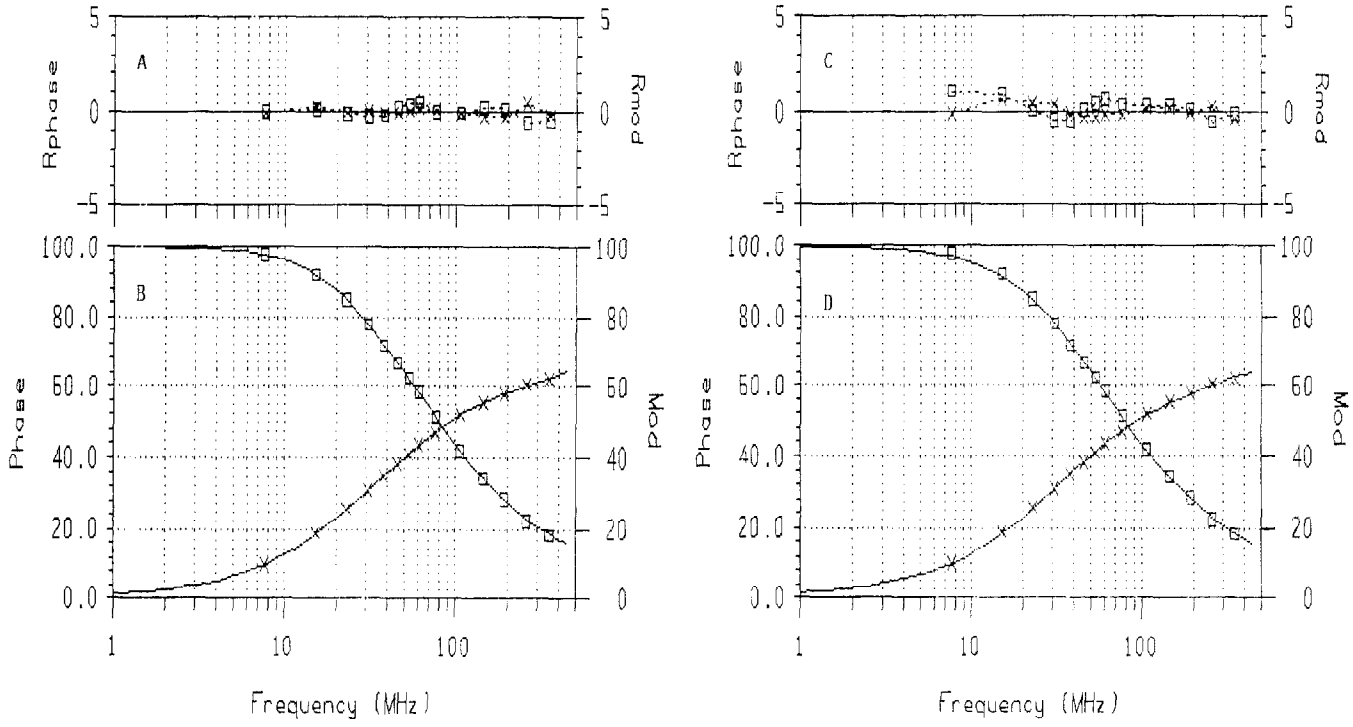

Fig. 1 Phase (crosses) and modulation (open squares) values for S-100a in the presence of 2 mM Ca^{2+} (**B**, **D**). Solid lines correspond to the best fits obtained using three exponentials (**B**) and two Lorentzian distributions of lifetimes (**D**). Superimposed (**A** and **C**) represent deviations between the calculated and the measured values of phase and modulation for the three exponential fit (**A**) and the two Lorentzian distributions of lifetimes (**C**).

measurement, the distribution widths of both lifetimes increased in presence of Ca^{2+} (+30% and +185% for longer and shorter lifetimes, respectively). The presence of Mg^{2+} did not change the Trp lifetime values and the associated fractional intensities (4.1 ns, 0.59 ns and f_1 = 0.40) but it increased the width of distribution associated with the longer component (+52%). In these conditions, Ca^{2+} did not significantly modify the centers of lifetime distribution (4.41 ns and 0.80 ns), but increased the fractional intensity associated with longer lifetime only to 57%. Also, the change in the width of distribution of lifetimes for both components was remarkable (–55.5% and

Table 3 Fluorescence decay fitting parameters for S100a in presence of PC sonicated vesicles. Fluorescence decay was measured at 18°C, with an excitation wavelength of 295 nm. When present, Ca^{2+} and Mg^{2+} were 2 mM and 5 mM, respectively. Final concentration of EPC SUV was 0.2 mM. Data were fitted to a sum of exponential decay components

	τ_1	f_1	τ_2	f_2	τ_3	f_3	X^2
No ions	1.07	1					1678
	3.87	0.51	0.48	0.49			23
	5.67	0.32	1.47	0.35	0.35	0.33	1.43
Ca^{2+}	2.66	1					1365
	4.30	0.82	0.55	0.18			32.3
	6.10	0.50	2.26	0.40	0.33	0.10	2.7
Mg^{2+}	1.17	1					1790
	4.35	0.51	0.49	0.53			24.4
	6.58	0.31	1.73	0.34	0.41	0.35	2.18
Mg^{2+} + Ca^{2+}	2.35	1					1620
	4.33	0.77	0.57	0.23			28.8
	5.80	0.52	1.99	0.35	0.36	0.13	4.94

τ_1, τ_2, τ_3 lifetime values (ns); f_1, f_2, f_3 fluorescence fractions; X^2, reduced chi-square. For other experimental details, *see* Materials and methods.

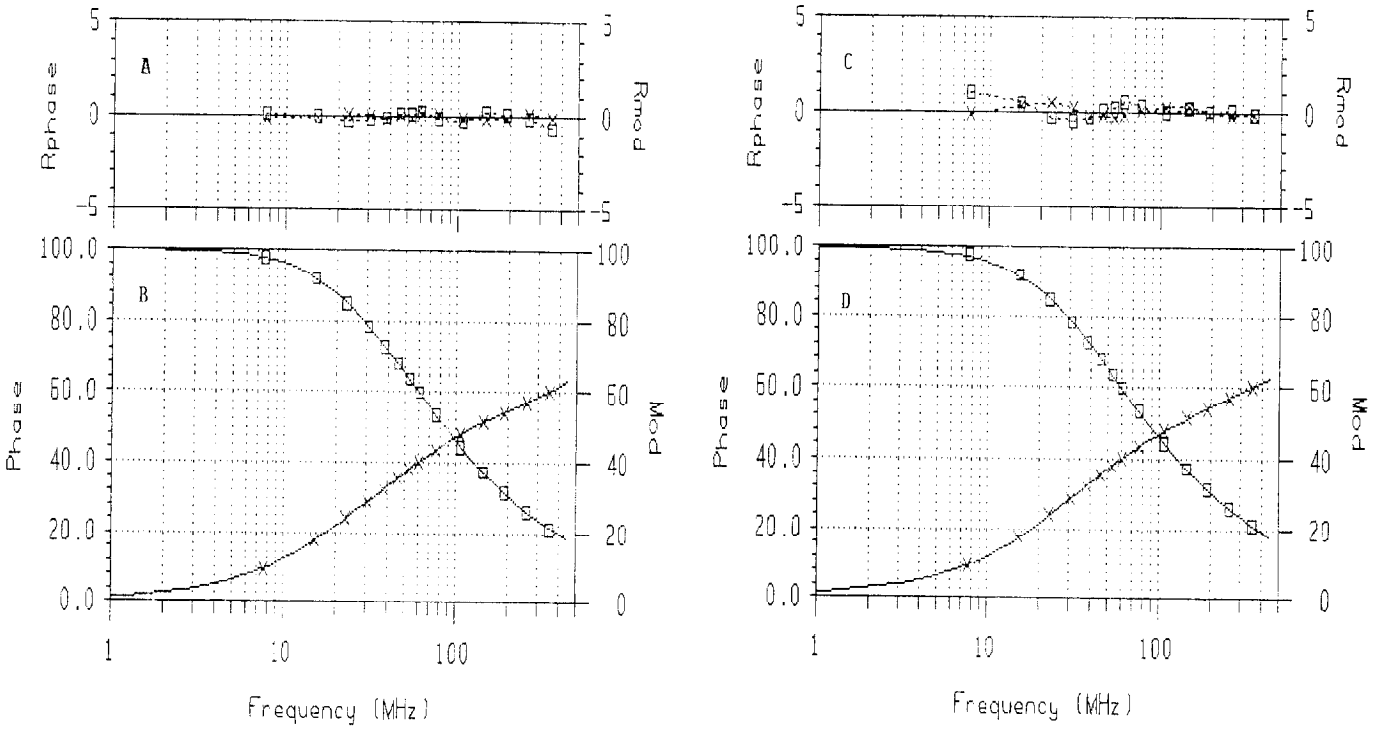

Fig. 2 Phase (crosses) and modulation (open squares) values for S-100a in the presence of 2 mM Ca^{2+} and 5 mM Mg^{2+} (**B**, **D**). Solid lines correspond to the best fits obtained using three exponentials (**B**) and two Lorentzian distributions of lifetimes (**D**). Superimposed (**A** and **C**) represent deviations between the calculated and the measured values of phase and modulation for the three exponential fit (**A**) and the two Lorentzian distributions of lifetimes (**C**).

+238%, respectively for longer and shorter lifetimes). The fluorescence decay of S-100a was measured also in the presence of EPC small unilamellar vesicles (SUV). SUV have been chosen because no osmotic volume changes have been reported for those minimal sized vesicles [16]. Tables 3 and 4 show the results obtained in the presence or in the absence of Ca^{2+} and/or Mg^{2+}.

Fluorescence decay of S-100a, in the presence of EPC SUV and in the absence of both Ca^{2+} and Mg^{2+}, is well described by three exponentials. Compared to S-100a in buffer (without Mg^{2+}), the exponential analysis showed only a small increase in the longer lifetime value (from 5.09 ns to 5.67 ns). No changes in the other lifetimes and in associated fractional intensities were detectable (Table 3). Similar modifications were obtained in the presence of Ca^{2+} or Mg^{2+}. The presence of both ions did not modify the exponential analysis of data. However, the two-component distributional analysis showed that liposomes

Table 4 Fluorescence decay fitting parameters for S100a in presence of PC sonicated vesicles. Fluorescence decay was measured at 18°C, with an excitation wavelength of 295 nm. When present, Ca^{2+} and Mg^{2+} were 2 mM and 5 mM, respectively. Final concentration of EPC SUV was 0.2 mM. Data were fitted as Lorentzian continuous distributions of lifetime values

	c_1	w_1	f_1	c_2	w_2	f_2	X^2
No ions	0.33	2.80	1				19
	4.04	1.63	0.41	0.54	0.69	0.59	1.37
+Ca^{2+}	2.63	4.48	1				62
	4.10	1.56	0.78	0.41	1.96	0.22	2.56
+Mg^{2+}	0.37	3.15	1				19
	4.01	2.63	0.48	0.58	0.49	0.52	0.74
+Mg^{2+} + Ca^{2+}	2.10	4.66	1				29
	4.48	0.96	0.62	0.74	2.03	0.38	3.10

f_1, f_2, f_3 fluorescence fractions; c_1, c_2, w_1, w_2, centers and widths of Lorentzian distributions, respectively; X^2, reduced chi-square. For other experimental details, *see* Materials and Methods.

actually affected the S-100a conformation. The interaction of S-100a with EPC slightly modified the fractional intensity linked to lifetimes, but largely increased the width of the distribution associated with the longer component (Table 4). This effect was also evident in the presence of divalent cations. No improvement of the fit was obtained, in all samples, by a three-component distribution analysis including a very short lifetime (0.001 ns), to eliminate light scattering contribution [13]. These data suggest that the interaction with the EPC SUV modifies the flexibility of the protein structure, changing the microheterogeneity of Trp environment or the rate of interconversion between subconformations.

Anisotropy decay measurements

Anisotropy decay parameters are shown in Table 5. Data were analyzed considering the fluorescence decay as arising from emitting species with lifetimes corresponding to the centers of bimodal Lorentzian distribution. The zero time anisotropy, calculated as $r_o = r_1 + r_2 = g_1r_o + g_2r_o$, is included in Table 5. Moreover, the anisotropy decay analyses were always performed also by using three lifetime values obtained by exponential analysis: results obtained were similar to those reported in Table 5, with higher X^2 values. Data were analysed allowing the total anisotropy to be a variable in the fitting algorithm, as previously described ([17] and references cited therein). The goodness of fit was judged by the value of reduced X^2. For the protein in buffer at 18°C, about 15.5% of recovered anisotropy was associated with a fast sub-nanosecond component, while the remaining anisotropy was associated with a rotational correlation time of 6.7 ns. The slow rotational correlation time is comparable to the value calculated for a rigid hydrated sphere of similar molecular weight, considering an hydration shell of 0.2 g/cm^3 [18]. Therefore, this component likely corresponds to the overall rotation of the protein in solution, while the fast component is most likely associated with local Trp motions within the protein matrix. The value of 0.31 for r_o, expected for Trp anisotropy in proteins in the range of excitation wavelength 270–300 nm [15], was completely recovered, indicating that motions in the protein were completely resolved by this analysis. After the addition of 2 mM Ca^{2+}, the short component disappeared while the longer component increased to 16.08 ns (g_1r_o = 0.210). This longer value of the rotational correlation time could have different explanations, such as a change in the protein shape or in the hydration shell. The possibility of protein aggregation also exists, however it was excluded in previous works performed in similar conditions [8,19]. The decrease in the value of recovered anisotropy is due to very fast motions of the Trp side chain, which cannot be resolved by our analysis. This hypothesis could explain the relatively high value of X^2 for this analysis. These results are in line with a higher flexibility of the part of polypeptide chain containing Trp, in the presence of Ca^{2+}. In this experiment, the use of a fixed value for total recovered anisotropy (r_o= 0.31) was attempted, because this condition enhances resolution of rapid correlation times [17]. However, no increase of number of ϕ values with an increase of fit was obtained in these conditions.

Under our experimental conditions, Mg^{2+} slightly increased the rotational correlation time associated with the overall rotation of the protein (9.26 ns), while the presence of this ion enhanced the increase in longer rotational correlation time caused by Ca^{2+} (33.75 ns) (Table 5). However, the analysis was unable to completely resolve the most rapid motions; in fact the apparent value of r_o was decreased to 0.282 and the X^2 is relatively high (Table 5). Although this hypothesis must be confirmed by other techniques, these data, together with the

Table 5 Anisotropy decay parameters for S100a. Measurements were performed in buffer (A) or in the presence of EPC vesicles (B)

	Sample	g_1r_o	ϕ_1	g_2r_o	ϕ_2	r_o	X^2
A							
	S100a	0.248	6.70	0.056	0.13	0.304	1.05
	+ Ca^{2+}	0.210	16.08	–	–	0.210	1.80
	+ Mg^{2+}	0.250	9.26	0.059	0.23	0.309	1.80
	+ Mg^{2+} + Ca^{2+}	0.201	33.75	0.077	0.68	0.278	2.70
B							
	S100a	0.139	13.85	0.168	0.20	0.307	1.70
	+ Ca^{2+}	0.137	19.01	–	–	0.137	3.70
	+ Mg^{2+}	0.179	8.85	0.064	3.40	0.243	2.10
	+ Mg^{2+} + Ca^{2+}	0.163	21.00	0.087	2.13	0.250	3.20

Data were acquired at 18°C using a λ_{ex} =295 nm. For other experimental details *see* Materials and Methods. r_o= time zero anisotropy; ϕ_1, ϕ_2 = rotational correlation times, in ns; r_1, r_2 = pre-exponential factors.

Lorentzian distributional analysis results, could be due to a possible change in the molecular shape. However, the possibility of an aggregation for the protein cannot be excluded, although previous studies [8], performed in similar conditions, did not describe this effect, but suggested that Mg^{2+} did not modify the effect of saturating concentrations of Ca^{2+}. Also, in this case, the use of the fixed value $r_0 = 0.31$ was attempted with unsatisfactory results. The same kind of analyses described were applied in samples containing lipids. In the presence of EPC SUV, about 45% of anisotropy was associated with a 13.85 ns component, while the remaining 55% decayed by segmental motions (0.2 ns). The value of rotational correlation time increased in the presence of Ca^{2+} (ϕ =19.01 ns, $r_0 = 0.137$). Also, in this case, the low value of r_0 suggests fast motions of Trp side chain, that was unresolved by our analysis. The presence of Mg^{2+} largely modified the anisotropy decay parameters in the presence of both EPC and EPC + Ca^{2+} (Table 5). The longer rotational correlation time is slightly decreased, as compared to the protein in the buffer (containing Mg^{2+}). However, about 26% of recovered anisotropy was associated with a 3.4 ns component. When both ions were present, the longer correlation time was 21 ns, and 35% of recovered anisotropy was associated with a 2.13 ns component.

DISCUSSION

Fluorescence decay lifetime of Trp residues can vary by more than a factor of 100 in different proteins [20]. The fluorescence decay of Trp is affected by several factors such as exposure to water, the presence of quenching moieties on the protein structure and/or excited state reactions. Trp emission decay in proteins is satisfactorily described by several exponential components, usually associated with different amino acid residues. However, also single Trp containing proteins can present complex decay, due to conformational heterogeneity [20]. Proteins can assume a large number of slightly different overall structures, called conformational substates [21]. The flexibility of the protein structure determines the heterogeneity of environments experienced by a fluorophore incorporated in a protein matrix during the excited state. Alcala et al. [22] described complex decays of Trp fluorescence in proteins by continuous lifetime distributions, demonstrating that also single Trp proteins can display a distribution of lifetimes, which could be ascribed to molecular or conformational heterogeneity. It was suggested that the width of lifetime distribution is related to the number of protein conformational substates and to the rate of interconversion between them [12]. To compare the present measurements with a previous work [13], fluorescence decay data of S-100a were analysed in terms of continuous Lorentzian lifetime distributions. We used the distribution fit as a more convenient way to directly compare the fits to data obtained for this protein. Results showing two relatively large distributions (centered around 3.90 ns and 0.55 ns) are related to a Trp experiencing a large number of microenvironments during its excited state lifetime, in agreement with our previous results [13]. Anisotropy decay data (Table 5) for the protein in buffer, showing a 6.7 ns long component, are consistent with predicted rotational correlation time for a globular protein of similar weight, with an hydration shell of 0.2 g/cm^3. The flexibility of the Trp environment is also shown by the association of 15% of recovered anisotropy with a short component. The Ca^{2+}-induced increase in the fractional intensity linked to longer fluorescence decay lifetime (75% compared to 35%: Table 1), was explained as a consequence of Ca^{2+}-induced increase in exposure to the solvent [13], causing a decrease in the internal dynamic quenching of the Trp-90 emission [14] or, alternatively, as a consequence of a reduction in Trp-90–Glu-91 interaction [15]. Moreover, the Ca^{2+}-dependent broadening of Trp lifetimes distribution (Table 2) can be related to a greater microheterogeneity of the environment sampled by Trp at 18°C. The presence of Ca^{2+} increases the rotational correlation time linked to the overall rotation of the molecule (16.08 ns). This increase could be a consequence of a change of the hydrodynamic shape of the protein, as suggested by Wang et al. [15]. Moreover, the low recovered anisotropy (0.210), is likely due to the presence of very fast motions of the indole ring, which cannot be resolved by our analysis. This is consistent with the hypothesis of a greater exposure of Trp residue to water, that decreases the possibility of interactions with neighbouring amino acid groups and causes, as a consequence, a greater motional freedom of the Trp indole ring and/or of the polypeptide chain containing this residue.

The small modifications associated with the presence of Mg^{2+} (Tables 1, 2 & 5) are in agreement with the small conformational changes induced by this ion on the Trp environment [14,15]. However the presence of Mg^{2+} greatly modifies the effect of Ca^{2+} on the Trp-90 environment, as indicated by fluorescence decay analysis (Tables 1 & 2). The decrease in Ca^{2+}-induced shift towards longer lifetime values is in agreement with previous data, suggesting a strong antagonistic effect exerted by Mg^{2+} on Ca^{2+} binding [8]. However, our data show a remarkable decrease in w_1 and, on the contrary, an increase in w_2. Although these data are not of easy interpretation, they suggest a Trp microenvironment structurally different from that presented by the protein in the presence of Ca^{2+} only. This hypothesis is supported by anisotropy decay data showing an increase in longer rotational correlation time, usually associated with a modification of the protein shape, while the value of the shorter component, linked

to segmental flexibility of the protein, suggests a reduced mobility of the environment containing the Trp residue in the presence of both ions. Although the possibility of an extensive aggregation of the protein could not be excluded, previous studies [8,19] did not describe this effect. The presence of Mg^{2+} was observed to result in a quite large decrease in the protein affinity for zinc and for Ca^{2+} [8]. These two ions interact with distinct binding sites on S-100 subunits [8]. It seems likely that Mg^{2+} binding to different negative sites on S-100a can modify, at least in part, some protein structural characteristics and, hence, the affinity of S-100a for these ions. In our samples, Mg^{2+} seems not to greatly change the binding characteristics of S-100a protein in the presence of excess Ca^{2+}, as suggested by the unmodified lifetime values and associated fractional intensities. However, the increase in rotational correlation time (from 9.26 ns to 33.75 ns) suggest a change in protein shape and flexibility. Also the observed modifications in w_1 and w_2 could be linked to modifications in protein shape. Recently, the three-dimensional structure of the S-100-like protein, calcyclin, has been determined in the apo state by NMR spectroscopy [23]. The ion-free calcyclin forms non-covalent dimers in which the two subunits are packed antiparallel to each other. The structures in contact in the calcyclin homodimer are helices IV and IV', and residues in helices I and I' also contribute to the dimer interface. Trp-90 in the α subunit of the S-100αβ heterodimer (S-100a) is preceded by Phe-89 which corresponds to Leu-88 in calcyclin [23]. In the latter protein, Leu-88 is suggested to make an important contribution, together with other hydrophobic residues, to the contact (hydrophobic) surface between the two calcyclin subunits [23]. Since the homodimeric fold described for calcyclin was suggested to apply to all members of the S-100 family except the short calbindin D_{9k} [23], we can assume that Phe-89 in S-100α plays the same role as Leu-88 in calcyclin. Whereas Leu-88 in calcyclin is followed by a basic residue (Lys-89), Phe-89 in S-100α is followed by the hydrophobic residue Trp-90. At present, we do not know what contribution Trp-90 in S-100α makes to the contact area in the S-100αβ heterodimer (S-100a) or in the S-100αα homodimer (S-100a_o), or whether Phe-89 in S-100α displays the same flexibility or accessibility as Trp-90 under the various experimental conditions employed in the present study. Our data indicate that Ca^{2+} causes an increase in the motional freedom of Trp-90, pointing to a greater accessibility of this residue to the solvent and to a relatively large change in the protein's shape. Although the Ca^{2+}-induced changes in S-100α are significantly reduced by the presence of Mg^{2+}, a certain degree of accessibility and flexibility is maintained when the protein is exposed to both ions. As the three-dimensional structure of Ca^{2+}, Mg^{2+}, or Ca^{2+}- Mg^{2+}-loaded calcyclin (or S-100α) has not yet been elucidated, one cannot draw definite conclusions concerning the extent of the Ca^{2+}, Mg^{2+}, or Ca^{2+}-Mg^{2+}-induced changes in the Trp-90 microenvironment. However, we speculate that Ca^{2+} and/or Mg^{2+} might produce changes in the extent of subunit association in S-100 dimers resulting in modifications of the three-dimensional structure of the cleft that is created upon dimer formation and is suggested to constitute a binding surface for S-100 target proteins [23]. In resting cells (i.e. at low free Ca^{2+} concentrations), S-100a is assumed to be in its Mg^{2+} conformation, which appear to be dissimilar from the S-100a conformation in the apo state on the basis of the present data. The (small) changes produced in S-100a by Mg^{2+} might induce the protein to associate with those targets, the interaction with which does not require the larger conformational change induced by Ca^{2+}. In at least one case, S-100a_o (αα) was shown to stimulate the adenylate cyclase activity in skeletal muscle cells in a Ca^{2+}-independent, Mg^{2+}-dependent manner [24]. After elevation of free Ca^{2+} concentration, S-100a would assume that Ca^{2+} (or Ca^{2+}/Mg^{2+}) conformation that enables the protein to interact with a number of target proteins (for reviews *see* [1–3]). The present observation that S-100a (and presumably most S-100 proteins) can assume different conformational substates in the presence of Ca^{2+} might contribute to explain the heterogeneity of target proteins of individual S-100 proteins as well as the target specificity in the cases of certain S-100 proteins [1–3,25]. The C-terminal extension of S-100α, that contains Phe-88, Phe-89 and Trp-90, has been reported to represent the binding site for TRTK-12 [26], a synthetic peptide derived from a sequence contained in the C-terminus of the α-subunit of the actin capping protein, CapZ [27]. This peptide was shown to bind to both S-100α and S-100β and to inhibit the binding of these S-100 subunits to CapZ [27,28], as well as the binding of both S-100α and S-100β to glial fibrillary acidic protein (GFAP) and their effects on GFAP assembly into type III intermediate filaments [29,30]. All the above events proved Ca^{2+}-dependent. In light of the data illustrated in the present report, we tentatively conclude that the binding of Ca^{2+} to S-100α (and S-100β) increases the accessibility of C-terminus of S-100α (and S-100β) to TRTK-12 and, hence, to CapZ α-subunit, GFAP and desmin, i.e. the S-100 target proteins so far shown to contain a sequence homologous to TRTK-12 [27,29,31]. However, we cannot exclude that other parts of S-100α molecule (e.g. the cleft that forms upon dimerization of S-100 subunits) might represent a binding surface for a number of S-100 target proteins. Availability of the synthetic peptide TRTK-12 could help to discriminate between different modes of S-100 interaction with its targets.

S-100 protein exists both in a cytoplasmic and in a membrane-associated form. Moreover, S-100 proteins can

interact in vitro with artificial and natural membranes that show remarkable modifications in their structural and functional properties upon S-100 binding [1]. However, the physiological role of these membrane-bound forms are far from being elucidated, although some experimental evidence suggests some important activity at the membrane level. For example, S-100a_0 ($\alpha\alpha$) can stimulate the adenylate cyclase activity in the absence of Ca^{2+} and in the presence of Mg^{2+}, whereas no effects of the protein on this enzyme were registered in the presence of both ions [24]. By contrast, S-100b ($\beta\beta$) was reported to inhibit the adenylate cyclase activity in the presence of Mg^{2+} and to stimulate it in the presence of Ca^{2+} [32]. Although the mechanism of action of these proteins on the adenylate cyclase activity was not elucidated, the possibility that they might affect the enzyme activity by perturbing the lipid environment of the adenylate cyclase complex cannot be excluded. For this reason, S-100a fluorescence decay was studied also in the presence of EPC SUV in the presence and the absence of divalent cations. In the presence of the lipid, both exponential and distributional analyses show a small shift towards longer lifetime values for S-100a fluorescence decay in each sample measured (compare Tables 1–4). In a previous work [13], we studied the interaction of S-100a with EPC multilamellar liposomes, at 20°C, using a similar lipid/protein molar ratio. The best fit was obtained with an unimodal distribution of lifetimes. We suggested that the absence of two distinct lifetimes could be due to the mobility of protein molecules, which is decreased by the interaction with the PL. The results in EPC multilamellar liposomes showed a decrease in the rotational mobility of the overall protein, without modifications of the average conformation around the Trp residue [13], although the rate of fluctuation of the protein was likely modified. In the present work, the fluorescence decay of S-100a in the presence of EPC SUV is satisfactorily described by a two components distributional analysis. The differences in the analysis of S-100a fluorescence decay in presence of SUV could be linked to structural differences between MLV and SUV [33,34], besides different experimental conditions in collecting data. Under these experimental conditions, the interaction of S-100a with liposomes results in an increase of the width of longer lifetime distribution (Lorentzian bimodal analysis, Table 4) together with an increase of the longer rotational correlation time (from 6.7 ns to 13.85 ns). These modifications are likely due to the interaction with the EPC SUV. The possibility of very fast motions in the protein structure, suggested by the low r_0 value, could be a consequence of a structural change in the protein. The interaction of S100 with EPC [35] and other liposomes was previously demonstrated ([10,11] and references cited therein). Moreover, it was suggested that the conformation of the protein and its Ca^{2+}-binding properties may vary depending on the types of phospholipids [10,11,13]. The present data may indicate that structural features of the lipidic membrane, i.e. the surface curvature, may be important for lipid induced structural modifications in S-100 protein. In the presence of EPC, the Ca^{2+}-induced changes in Trp fluorescence and anisotropy decay are not modified, although the lifetime distribution remain broad. These results show that the lipid-induced increase in the protein conformational microheterogeneity does not change the Ca^{2+} effects on the Trp microenvironment, in the absence of Mg^{2+}. However, data obtained in the presence of Mg^{2+} indicate some interaction between lipids and S-100, likely mediated by this ion, although other experiments are necessary to elucidate the degree and the kind of interaction between the protein and the lipid in these conditions. Yet, the present observations indicate that S-100 association with membranes might represent a means to concentrate S-100 proteins at specific sites in a conformation suitable for the regulation of membrane activities.

ACKNOWLEDGEMENTS

This work was supported by CNR funds to GZ No. 92.03589, CNR to GC No.93.00252, NIH R41 to EG and Telethon (Italy) funds to RD.

REFERENCES

1. Donato R. Perspectives in S-100 protein biology. *Cell Calcium* 1991; **12**: 713–726.
2. Zimmer D.B., Cornwall E.Y., Landar A., Song W. The S-100 protein family: history, function and expression. *Brain Res Bull* 1995; **37**: 417–429.
3. Schaefer B.W., Heizmann C.W. The S-100 family of EF-hand calcium-binding proteins: function and pathology. *Trends Biochem Sci* 1996; **21**: 134–140.
4. Isobe T., Okuyama T. The amino acid sequence of the α-subunit in bovine brain S-100a protein. *Eur J Biochem* 1981; **116**: 79–86.
5. Baudier J. Gerard D. Ion binding to S100 proteins. II. Conformational studies on calcium-induced conformational changes in S100αα protein: the effect of acidic pH and calcium incubation on subunit exchange in S100a (αβ) protein. *J Biol Chem* 1986; **261**: 8204–8212.
6. Mani R.S., Kay C.M. Isolation and spectral studies on the calcium binding properties of bovine brain S-100a protein. *Biochemistry* 1983; **22**: 3902–3907.
7. Baudier J., Gerard D. Ions binding to S100 proteins: structural changes induced by calcium and zinc on S100a and S100b proteins. *Biochemistry* 1983; **22**: 3360–3369.
8. Baudier J., Glasser N., Gerard D. Ions binding to S100 proteins. *J Biol Chem* 1986; **261**: 8192–8203.
9. Donato R. S-100 proteins. *Cell Calcium* 1986; **7**: 123–145.
10. Zolese G., Tangorra A., Curatola G., Giambanco I., Donato R. Interaction of S-100b protein with cardiolipin vesicles as monitored by electron spin resonance, pyrene fluorescence and circular dichroism. *Cell Calcium* 1988; **9**: 149–157.
11. Zolese G., Curatola G., Amati S., Giambanco I., Donato R. S-100b protein regulates aggregation and fusion of cardiolipin vesicles.

Cell Calcium 1990; **11**: 35–46.
12. Alcala J.R., Gratton E., Prendergast F.G. Resolvability of fluorescence lifetime distributions using phase fluorometry. *Biophys J* 1987; **51**: 587–596.
13. Zolese G., Giambanco I., Curatola G., De Stasio G. Donato R. Time-resolved fluorescence of S-100a protein in the absence and presence of calcium and phospholipids. *Biochim Biophys Acta* 1993; **1162**: 47–53.
14. Baudier J., Tyrzk J., Lofroth J.E. Lianow P. A subnanosecond pulse fluorometric study of the Ca^{2+} and Mg^{2+} induced conformational changes on S-100a protein. *Biochem Biophys Res Commun* 1984; **123**: 959–965.
15. Wang C-K., Mani R.S., Kay C.M., Cheung H.C. Conformation and dynamics of bovine brain S-100a protein determined by fluorescence spectroscopy. *Biochemistry* 1992; **31**: 4289–4295.
16. de Gier J. Osmotic behaviour and permeability properties of liposomes. *Chem Phys Lipids* 1993; **64**: 187–196.
17. Lakowicz J.R., Laczko G., Gryczynski I., Cherek H. Measurement of subnanosecond anisotropy decays of protein fluorescence using frequency-domain fluorometry. *J Biol Chem* 1986; **261**, 2240–2245.
18. Munro I., Pecht I., Stryer L. Subnanosecond motions of tryptophan residues in proteins. *Proc Natl Acad Sci USA* 1979; **76**: 56–60.
19. Mani R.S., Kay C.M. Hydrodynamic properties of bovine brain S-100 proteins. *FEBS Lett* 1984; **166**: 258–262.
20. Beechem J.M., Brand L. Time-resolved fluorescence of proteins. *Annu Rev Biochem* 1985; **54**: 43–71.
21. Frauenfelder H., Parak F., Young R.D. *Annu Rev Biophys Biophys Chem* 1988; **17**: 451–479.
22. Alcala J.R., Gratton E., Prendergast F.G. Fluorescence lifetime distributions in proteins. *Biophys J* 1987; **51**: 597–604.
23. Potts B.C.M., Smith J., Akke M. et al. The structure of calcyclin reveals a novel homodimeric fold for S-100 Ca^{2+}-binding proteins. *Nature Struct Biol* 1995; **2**: 790–796.
24. Fanò G., Angelella P., Meriggiò D., Aisa M.C., Giambanco I. Donato R. S-$100a_0$ protein stimulates the basal (Mg^{2+}-activated) adenylate cyclase activity associated with skeletal muscle membranes. *FEBS Lett* 1989; **248**: 9–12.
25. Garbuglia M., Verzini M., Giambanco I., Spreca A., Donato R. Effects of calcium-binding proteins (S-$100a_0$, S-100a, S-100b) on desmin assembly in vitro. *FASEB J* 1996; B1:, 317–324.
26. Osterloh D., Ivanenkov V.V., Schaefer B.W., Heizmann C.W., Gerke V. Hydrophobic residues in the C-terminal extension of the S-100α (S-100A1) molecule are involved in ligand binding. Proc. *Fourth European Symposium on Calcium Binding Proteins in Normal and Transformed Cells*, Perugia, Italy, May 2–5, 1996, P107
27. Ivanenkov V.V., Jamieson Jr G.A., Gruenstein E., Dimlich R.V.W. Characterization of S-100b epitopes. Identification of a novel target, the actin capping protein, CapZ. *J Biol Chem* 1995; **270**: 14651–14658.
28. Ivanenkov V.V., Dimlich R.V.W., Jamieson Jr G.A. Interaction of S-$100a_0$ protein with actin capping protein, CapZ: characterization of a putative S-$100a_0$ binding site in CapZ α-subunit. *Biochem Biophys Res Commun* 1996; **221**: 46–50.
29. Bianchi R., Garbuglia M., Verzini M. et al. S-100 (α and β)-binding peptide (TRTK-12) blocks S-100/GFAP interaction: identification of a putative S-100 target epitope within the head domain of GFAP. *Biochim Biophys Acta* 1996; In press.
30. Bianchi R., Giambanco I., Donato R. S-100 protein, but not calmodulin, binds to and inhibits the polymerization of the glial fibrillary acidic protein in a Ca^{2+}-dependent manner. *J Biol Chem* 1993; **268**: 12669–12674.
31. Garbuglia M., Verzini M., Dimlich R.V.W., Jamieson Jr G.A., Donato R. Characterization of type III intermediate filament regulatory protein target epitopes: S-100 (β and/or α) binds the N-terminal head domain; annexin II_2–$p11_2$ binds to rod domain. *Biochim Biophys Acta* 1996; In press.
32. Fanò G., Della Torre G., Giambanco I., Aisa M.C., Donato R., Calissano P. S-100b protein stimulates the activity of skeletal muscle adenylate cyclase in vitro. *FEBS Lett* 1988; **240**: 177–180.
33. Fenske D.B. Structural and motional properties of vesicles as revealed by nuclear magnetic resonance. *Chem Phys Lipids* 1993; **64**: 143–162.
34. Winterhalter M., Lasic D.D. Liposome stability and formation: experimental parameters and theories on the size distribution. *Chem Phys Lipids* 1993; **64**: 35–43.
35. Calissano P., Alemà S., Fasella P. Interaction of S-100 protein with cations and liposomes. *Biochemistry* 1974; **13**: 4553–4560.